Conf-9406213--3

LA-UR- 93-4436

Title: NATURE OF DISSOLUTION OF BINARY TANTALUM-TITANIUM ALLOYS BY MOLTEN PLUTONIUM

Author(s):
J.D. Cotton, MTL-6
K.M. Axler, NMT-3
P.C. Lopez, NMT-3
H.H. Steele, NMT-5
J.I. Archuleta, NMT-5

Submitted to:
1994 TMS Meeting
San Francisco, CA
February 27-March 3, 1994

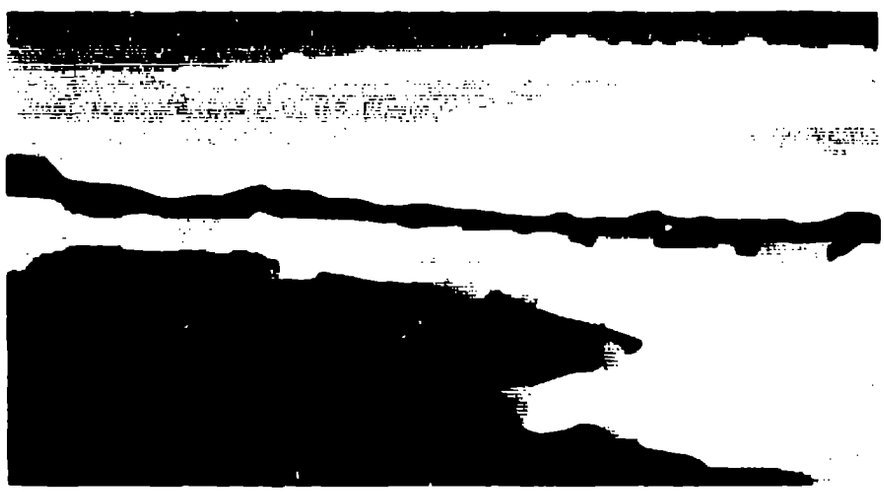

Los Alamos
NATIONAL LABORATORY

NATURE OF DISSOLUTION OF BINARY TANTALUM-TITANIUM ALLOYS BY MOLTEN PLUTONIUM

J.D. Cotton, K.M. Axler, P.C. Lopez, J.H. Steele and J.I Archuleta

Los Alamos National Laboratory
Los Alamos, New Mexico 87545

Abstract

Tantalum hardware has often been used for the processing of molten Pu where ceramics are inappropriate. However, there has only been limited work on the containment of Pu by Ta alloys. In this regard, we have investigated the interaction of Ta-Ti alloys (20, 40 and 60 wt.% Ti) with molten Pu at 850 and 1000 °C. The microstructures of Pu/alloy interfaces were characterized chemically and metallographically following various exposures to liquid Pu. Dissolution does not proceed uniformly, but appears to initiate by intergranular attack to a shallow depth and then progress by the formation of a stable mushy zone at the liquid/solid interface. The resistance to dissolution by molten Pu increases with the Ta content of the alloy.

This work was funded by the Department of Energy under contract #W-7405-ENG-36.

Introduction

The refractory metals (Nb, Mo, Ta and W) are well known for their ability to contain liquid metals with minimal property degradation. This is largely a result of their high melting points, which produce low diffusion rates, the absence of intermediate phases, and low mutual solubilities with respect to typical liquid metals. However, some of these same properties also increase difficulty in processing. In addition, the high densities and poor oxidation resistance of refractory metals may limit their range of application. Such issues can be addressed by certain alloying additions, although usually at some property cost. It is the balance of such costs that comprises the focus of this study which deals with the problem of containment of molten Pu metal.

Thermochemical processing of Pu often requires the metal be contained in the liquid state at temperatures ranging several hundred degrees above the melting point. A suite of alloy containment materials for liquid Pu has been previously investigated (1-4). Metallic processing hardware and containers are usually comprised of Ta or Ta-based materials due to its inherent resistance to attack (1,5). Nonetheless, the high melting point of Ta, combined with its poor machinability and low oxidation resistance make it less than ideal for certain applications. In an effort to improve these properties, Ti was chosen as an alloying addition. The rational for choosing Ti includes better processing characteristics, improved oxidation resistance, lower density and lower cost.

Upon adding Ti, the processing characteristics of Ta are improved largely as a result of the reduction in melting point, as shown by the binary phase diagram in Figure 1 (6). For example, the solidus temperature of 80 wt.% Ta-20 wt.% Ti is 2230 °C, nearly 800 °C lower than that of pure Ta. This decrease in solidus temperature allows casting to be performed with greater ease. And contrary to the often observed embrittling effect of solute additions to refractory metals, there is little sacrifice in ductility due to the addition of Ti (7,8). Another advantage is the marked reduction in density, a result of the large disparity in densities of the parent metals (4.5 g/cc for Ti versus 16.6 for Ta). A notable improvement in oxidation resistance also occurs on adding Ti to Ta (8-12) which not only assists in processing, but opens other possibilities for more durable Pu processing hardware.

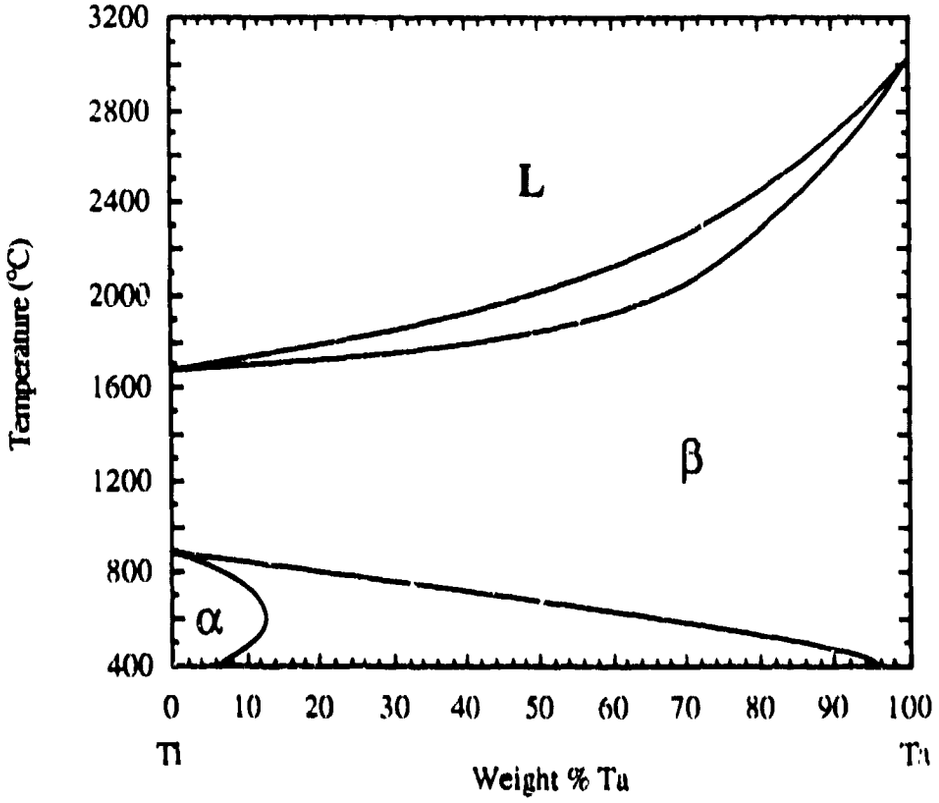

Figure 1. Binary Phase Diagram for the Ti-Ta System.

All the above factors suggest that Ti would be an attractive addition to Ta. However, the ability of the resulting alloy(s) to effectively contain Pu liquid is unknown. A number of intrinsic factors control the ability of a metal or alloy to resist dissolution by a metallic liquid. These include: intersolubilities of the containment material and the liquid metal, interfacial reactions, grain size, diffusivities in the different phases, prior retained work (dislocation density), and the distribution of second phases. Of these, one of the most important factors is the solubility of the containment material in the liquid, since this provides the overall driving force for dissolution. In fact, as noted above, one of the principal reasons for the use of refractory materials for liquid metal containment is their low solubility in the liquid metals they are chosen to contain. The solubility of a number of refractory and other high melting point metals in liquid Pu at 1000 °C is shown in Table I (13,14).

Table I. Solubility of Selected Metals in Liquid Pu at 1000 °C.

Metal	Solubility (at.%)
W	0.05
Ta	0.5
Nb	3.7
Re	4.5
V	4.5
Mo	5.1
Cr	8.7
Zr	24.4
Ti	37.1

Aside from W, Ta is an excellent choice for Pu thermochemical processing hardware, based on solubility alone. However, by comparison W is more difficult to fabricate and is essentially unweldable; it will not be considered further. On the other hand, Ti is predicted to be one of the least effective metals to contain molten Pu, in spite of the beneficial effects on Ta described above. Thus, several questions are raised as to the effectiveness of a Ta-Ti alloy in containing Pu. How does it vary with composition? What is the effect of microstructure? How does dissolution progress? These are addressed in this study and presented below.

Experimental Procedures

Alloy and Specimen Fabrication

Alloys containing 40, 60 and 80 wt.% Ta, balance Ti, were produced by conventional arc melting 16 100 gm buttons of the intended composition and remelting each twice more; all the buttons were then melted together into a large rectangular slab approximately 1.5 cm thick. Starting materials were Ti crystal bar (99.9 % purity) and Ta sheet of commercial purity. The 40 and 60 wt.% Ta slabs were soaked at 930 °C for 1 hour under flowing argon gas prior to hot rolling utilizing multiple passes. Upon reaching a thickness of approximately 0.2 cm the sheet was allowed to cool to room temperature. The 80 wt.% Ta alloy was processed similarly at 1100 °C. Chemical analysis by X-ray fluorescence of representative samples of each slab indicated that the 40 and 60 wt.% Ta alloys were within one percent of intended composition and that the 80 wt.% Ta alloy was approximately 2 wt.% richer in Ta, presumably due to losses during melting and casting. Disks, 2.0 cm in dia., were mechanically punched from the rolled sheets. These were ground on 400 grit SiC paper to remove surface oxide and α case. Final thicknesses ranged from 0.15 to 0.18 cm. Each specimen was cleaned ultrasonically by an organic solvent to remove surface contamination prior to testing.

Corrosion Tests and Analyses

Coupon Test. An initial test was conducted by placing a Ta-60 wt.% Ti coupon in a MgO crucible with a small amount of Pu and heating to 850 °C under commercial purity argon gas.

The heating and cooling rates were not monitored. Following two hours exposure the crucible was allowed to cool to room temperature. The test pieces are shown in Figure 2 following the exposure.

Figure 2. Ta-60 wt.% Ti coupon with Pu and MgO crucible used in compatibility test.

Flat Plat Tests. Additional tests were conducted by enclosing the Pu in a vertical MgO cylinder placed on disks of each binary composition. The disk was set into a concentric recess in a MgO ring and sealed about the edges with ZrO_2 cement, which was given a low temperature bakeout to set. See the schematic in Figure 3. For these tests, the Pu liquid volume/exposed alloy surface area (V/A) was 1.9 cm in each case. The tests were conducted under vacuum at 1000 °C for 2 hrs. The time required for the liquid Pu to reach 1000 °C and to later solidify was approximately 10 min. in each case.

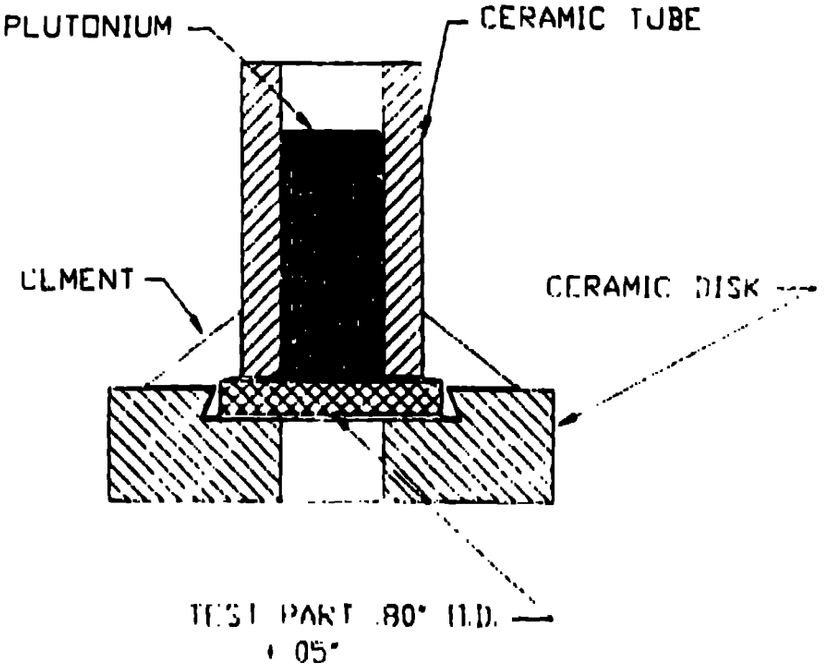

Figure 3. Schematic of Flat Plate Corrosion Test Apparatus

The specimens were characterized taking appropriate metallographic sections and analyzing by optical and scanning electron microscopy (SEM) combined with electron microprobe analysis (EMPA). By these techniques the corrosion penetration depth, phases present, and mode of attack were studied.

Results and Discussion

Coupon Test of Ta-60 wt.% Ti. The Ta-60 wt.% Ti coupon with solidified Pu and MgO crucible are shown in Figure 2 following the initial test. From this figure, it is apparent that the Pu did not completely flow around the specimen as expected, although the furnace temperature was well above its melting point. This suggests that the Pu surface oxide had inhibited flow of the liquid metal. Both optical metallography and microprobe analysis were utilized to investigate further the degree of interaction between the Pu and alloy.

A cross section through the test piece is shown in Figure 4. This figure shows that attack was more advanced at the location of the Pu and also that the Pu liquid wetted the entire surface of the test specimen forming a layer approximately 150 μm thick. Closer examination (Figure 5) of the Pu/alloy interface at the wetted layer reveals two distinct regions of attack. Attack immediately adjacent the Pu liquid occurred by localized penetration of the microstructure to leave rounded "globules" of Ta-Ti alloy. These globules are smaller than the grain size of the material. The initial attack into the material occurred intergranularly to a distance of about one or two grain diameters.

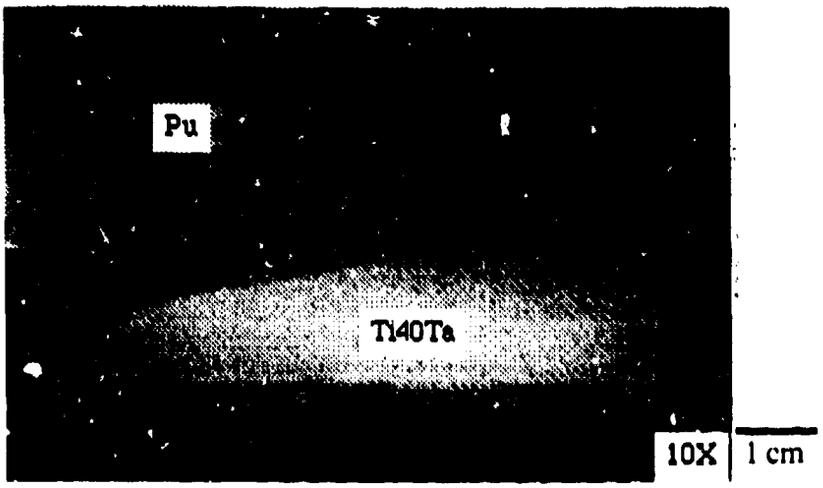

Figure 4. Optical Micrograph of Cross-Section Through Ta-60 Wt.% Ti Coupon with Pu

X-ray maps were constructed during microprobe analysis for Pu, Ta and Ti (Figure 6). These show that Pu is concentrated between the globules and along grain boundaries. Chemical spot analyses by EMPA further showed that the material along these boundaries has a composition of 97.8 Pu, 1.9 Ti and 0.3 Ta (wt.%). As the equilibrium binary solubilities of Ti and Ta in Pu at 850 °C are 6.6 and 0.15 wt.%, respectively (13,14), this suggests that Ta reduces the solubility of Ti in liquid Pu, while Ti increases the solubility of Ta in liquid Pu. The X-ray map for Ti also shows that Ti solute has built up in a boundary layer in the adjacent liquid Pu to a concentration greater than in the nearby globules of alloy whereas the Ta content in this region was essentially zero. This was also confirmed by X ray linescan (Figure 7). Approximately 0.08 wt.% Pu was detected throughout the alloy cross section. If one assumes this was not an artifact of metallographic preparation, it suggests a rather high diffusivity of Pu in this alloy under these conditions.

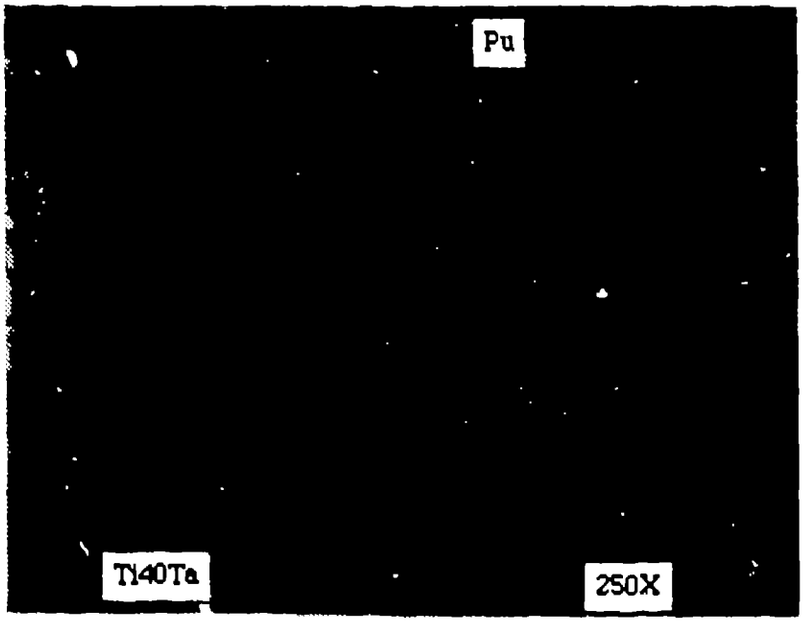

Figure 5. Optical Micrograph of the Pu/Ta-60 Wt.% Ti Interface.

Figure 6. Backscattered Electron Image (Upper Left) and X-ray Maps for Pu, Ti and Ta Across the Pu/Ta-60 Wt.% Ti Interface. Pu is to the right, alloy base metal to the left.

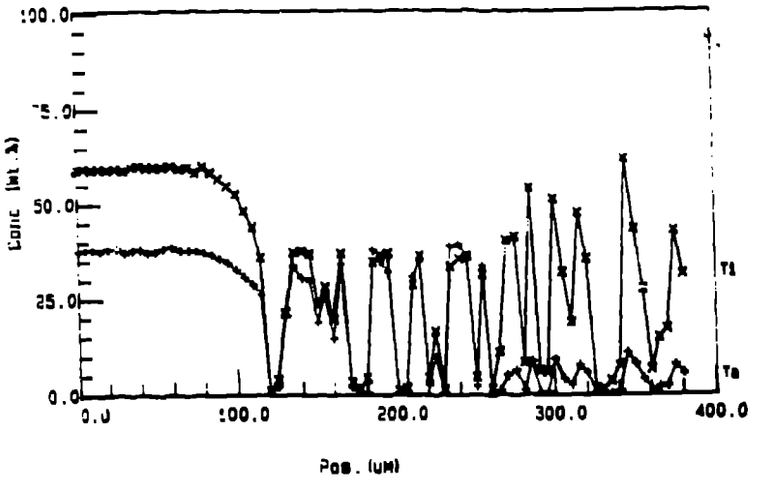

(a)

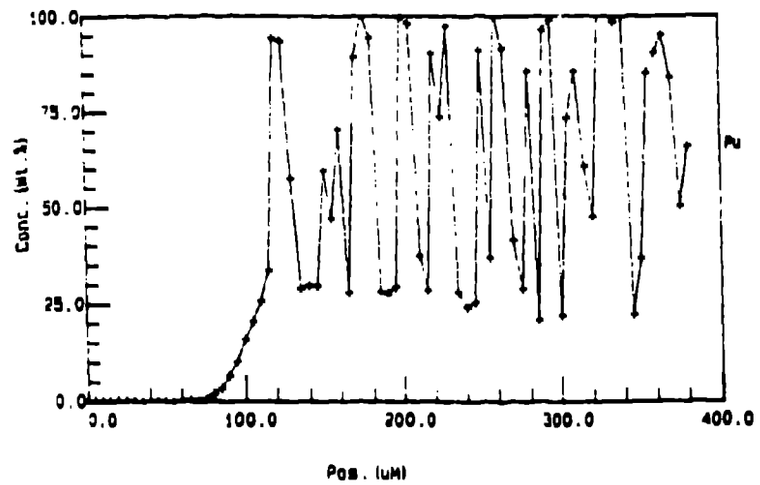

(b)

Figure 7. X-ray Linescans for Ti and Ta (a), and Pu (b) at the Ta-60 Wt.% Ti/Pu Interface Following 850 °C/2 hr Exposure.

The results of the spot chemical analyses are summarized in Table II. Pu-rich boundaries are the Pu-rich regions between the globules and are likely representative of the grain boundary regions farther into the specimen matrix as well. The low total percentage of elements in the outer Pu layer likely indicates the presence of Pu oxides.

Table II. Microprobe Chemical Analyses (Wt.%)

Location	Ti	Ta	Pu	Total
Ta-Ti alloy matrix	59.6	37.9	0.08	97.6
Ta-Ti globules	38.2	31.9	29.6	99.7
Pu-rich boundaries	2.0	0.3	98.1	100.3
Outer Pu layer	1.49	0	94.6	96.1

One of the most important results of this initial experiment is that Ta appears to have reduced the solubility of Ti in liquid Pu by factor of three (14), although this is a tentative result since the cooling rate from 850 °C is unknown. Since the rate of dissolution is proportional to the solubility in liquid metal (15), the best choice of containment materials are those with low solubilities in liquid Pu at the temperature of interest. Therefore, if the solubility of Ti can be

reduced, the attack rate may be reduced also. Furthermore, even though the solubility of Ta in liquid Pu has increased by about a factor of two due to the presence of Ti (13), the fact that it is inherently low, and its atom proportion in this alloy is small (15 at.%), suggests that this effect is less important than the change in Ti solubility.

However, a decreased solubility in itself is insufficient to reduce corrosion if the mode of attack is localized, e.g. at grain boundaries. The initial stages of dissolution take place at the grain boundaries. This is logical, since the grain boundaries are of a higher energy than the bulk and has been observed in pure Ta corrosion tests (1). However, the total penetration along the grain boundaries is limited to about two grain diameters after which the Pu-encased grains are heterogeneously dissolved. The source of this mode of attack is perplexing, since there is no obvious microstructural feature with which it corresponds. The scale of this attack is certainly smaller than the grain size of the bulk. Therefore, the grain boundaries cannot be the source of the dissolution paths. Neither can it be subgrains, since related investigations have revealed a relatively dislocation free microstructure. One possibility is the presence of Ta-lean regions which are the prior locations of α precipitates. However, these would be expected to be homogenized within the time frame of the test and, since there is no visible change in the mode of attack with increasing depth, this is unlikely.

Flat Plate Corrosion Tests of Ta-20, -40 and -60 Wt.% Ti. Low magnification photomicrographs of vertical sections through representative test specimens are shown in Figure 8. The solidified column of Pu is still attached. The region of attack can be discerned as a dark area immediately adjacent the Pu and of similar contrast. Comparison of the photomicrographs in Figure 8 show immediately that the extent of attack varies inversely with Ta content, as expected. The retention of the original interface is surprising, given the disparate densities of the alloy (6.2 g/cc) and liquid Pu (16.6 g/cc). That is, the less dense alloy constituents would be expected to rise in the liquid and also to create convention currents. However, if Ti is preferentially removed from the Ti-Ta alloy while Pu is taken up, as shown by the EMPA results, the resulting density of the "globules" of alloy remaining will be greater than that of the original alloy. This may help explain the interfacial stability observed. There may also be some degree of mechanical interlocking between the remnants of the Ta-Ti alloy microstructures.

A SEM examination of the regions of attack provided a more careful measurement of the attack depth in each specimen (Figure 9). The measured attack depths are plotted as a function of composition in Figure 10. These measurements represent the maximum depth at which a visible material change was observed.

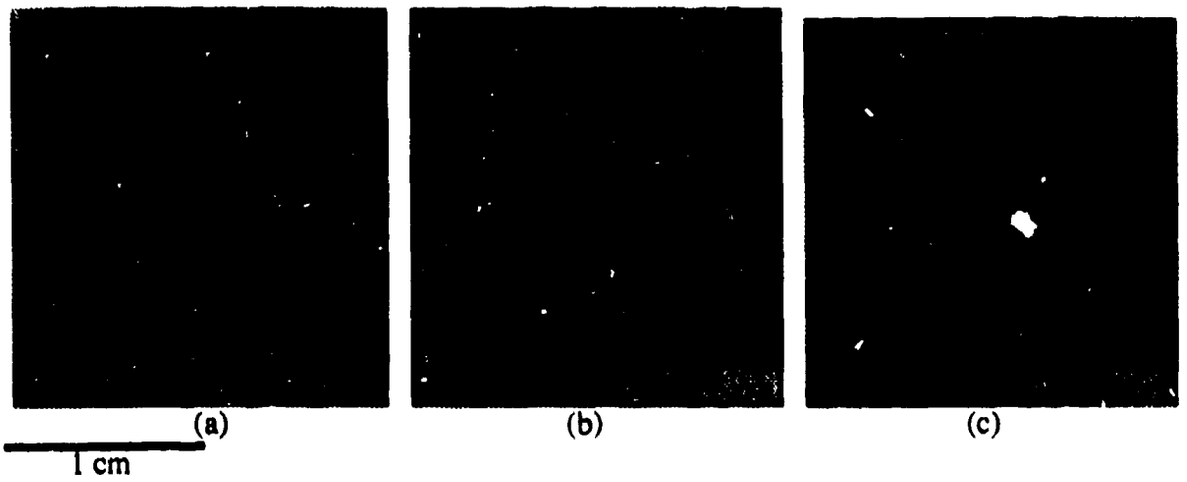

Figure 8. Typical Optical Photomicrographs of Vertical Sections Through Column of Solidified Pu and Ta-Ti Alloy Disks: (a) Ta-60 wt.% Ti; (b) Ta-40 wt.% Ti; (c) Ta-20 wt.% Ti. Evidence of attack is visible in the regions adjacent the Pu.

(a)

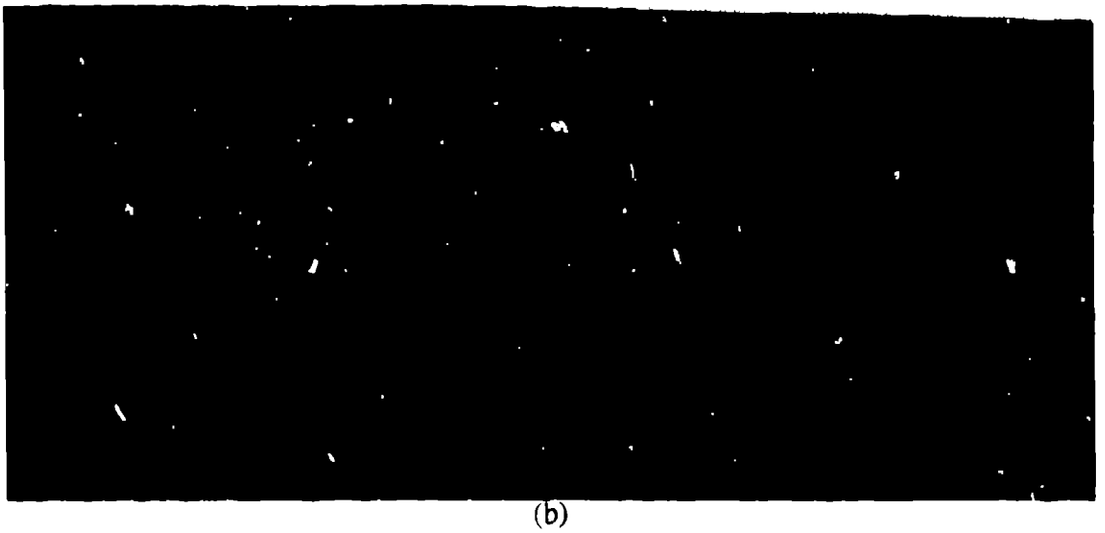

(b)

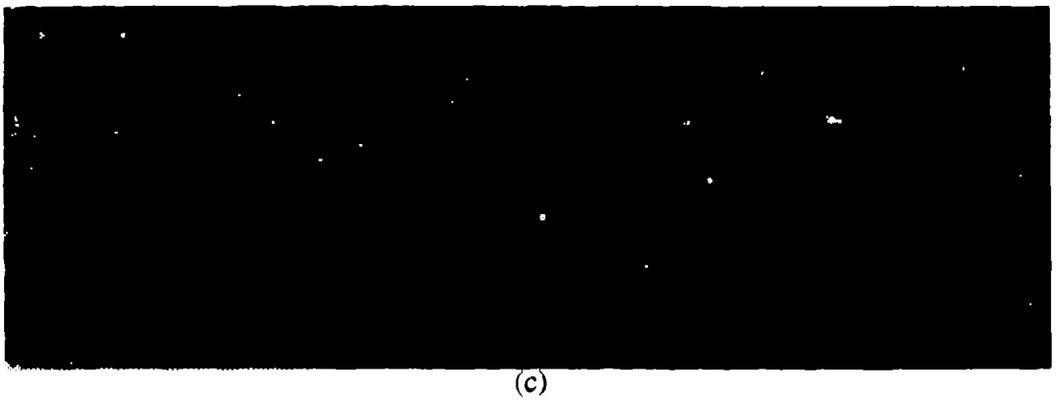

(c)

1 μm

Figure 9. Scanning Electron Micrographs of the Pu/Ta-Ti Interface: (a) Ta-60 wt.% Ti; (b) Ta-40 wt.% Ti; (c) Ta-20 wt.% Ti. The figures have been rotated 90 degrees CCW for publication (up is left, down is right).

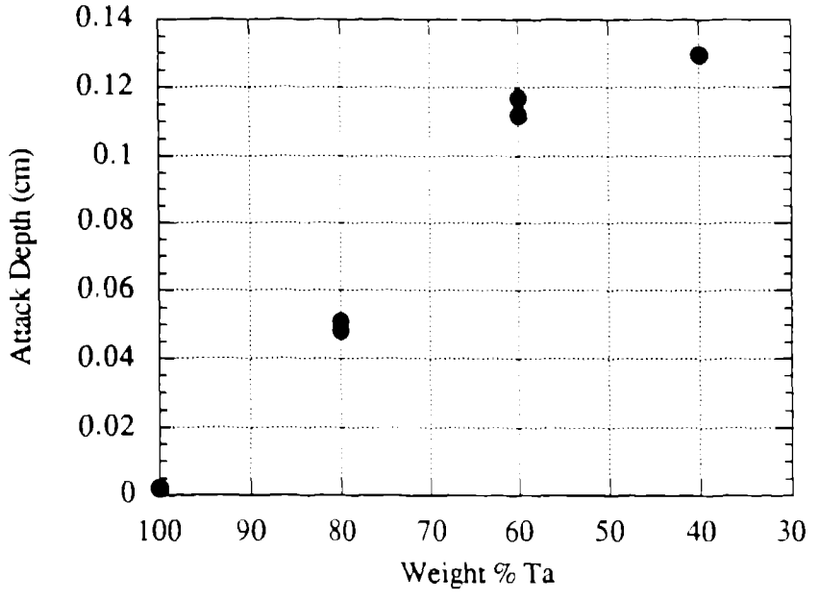

Figure 10. Depth of Attack of Ta-Ti Alloys by Molten Pu During 2 Hrs at 1000 °C in Vacuum as a Function of Composition. The value for pure Ta is from (1).

A number of observations can be made based on Figures 9 and 10.

1. The depth of attack depends on composition.

2. The scale of attack also varies with composition. That is, the size of the alloy debris (globules) decreases while their volume fraction increases with increasing Ta content.

3. Remnants of the original Ta-Ti alloy microstructure are maintained. The grain boundaries remain visible.

4. Initial attack progresses intergranularly, but only for a short distance, about 200 μm.

5. Grain dissolution is heterogeneous. No grains appear to dissolve completely. Rather, the proportion of alloy remaining decreases as the Pu is approached, causing the globules of alloy to appear finer. This is most obvious in the Ta-60 wt.% Ti alloy.

The depth of attack decreases with increasing Ta content, as intuitively expected based on the relative solubilities of Ti and Ta in liquid Pu, Table I. However, implicit in this expectation is the assumption that Ta will saturate the liquid (reach its binary solubility limit) at about the same solute level as in the binary system. Based on this assumption, the alloy attack depth will be a factor of (100/at.% Ta) relative to pure Ta. For example, an alloy containing 50 at.% Ta (~80 wt.% Ta) would be predicted to experience an attack depth of twice that for pure Ta. As can be seen in Figure 10 above, the actual attack depth is several times this level.

This comparison shows that attack depths cannot be predicted based on Ta content alone; other factors are also important. As shown by the microprobe analysis of the Pu in the grain boundaries (Table II), the solute levels in the Pu are not dictated by the equilibrium solubilities of the binary Pu-Ti and Pu-Ta systems. Therefore, the ternary solubility of the (Ta,Ti) alloy must deviate significantly from the linear interpolation of the solvus compositions of the binary

diagrams. The kinetic limitations must also be considered since longer times at temperature would be required to approach equilibrium and a slow cooling rate would cause some changes in the solute levels.

Another microstructural difference is grain size, which varies inversely with Ta content for the binary alloys processed in this study. This is largely a result of the different recrystallization temperatures of the alloys. Based on the hot rolling schedules described above, the Ta-60 wt.% Ti alloy is expected to be fully recrystallized, the Ta-40 wt.% Ti alloy partially recrystallized, and the Ta-20 wt.% Ti alloy unrecrystallized (8). Since the grain boundary area is roughly proportional to the square of the grain size, and corrosion appears to initiate at the grain boundaries, this could help account for the large difference in corrosion behavior between the three alloys. In fact, a significant increase in the corrosion rate was observed by Andelin, Kirkbride and Perkins by increasing the grain size of pure Ta via high temperature anneals (1).

The alloys also differ in their propensity for second phase precipitation at lower temperatures. Although all compositions in the Ta-Ta system are expected to be single phase β at the test temperature (Figure 1), precipitation of hexagonal α during the air cool following the hot rolling operation occurs for Ta-60 wt.% Ti in the form of 1 μm particles (16). The maximum solubility of Ta in the α phase is only about 3 at.%. Although the α precipitates will revert to β immediately on exceeding the β transus temperature, the regions of low Ta content would remain until adequately homogenized. Thus, at the beginning of the test, regions of high Ti content would be present and be preferred locations for attack. Nonetheless, the present evidence makes such a scenario unlikely, since the Ta-40 wt.% Ti behaves similarly yet has essentially no α precipitates and, as observed above, there is no change in the mode of attack during the course of the test. In addition, the regions of localized attack in Figure 8a are much larger than the prior α precipitates. Therefore, the presence of second phase cannot account for the heterogeneous nature of the dissolution of the free grains.

Aspects of the materials' behavior remain undefined, particularly the retention of the "skeletal" alloy microstructure in what appears to be a mushy zone during the test. The mechanical stability of this zone must be a result of some degree of mechanical interlocking of feature of the prior microstructure. Otherwise, the differences in density would cause disintegration of the interface zone. The EMPA results indicate that little solute actually enters the bulk Pu liquid. This suggests that the liquid within the mushy zone is quiescent and perhaps that solute transport through the liquid in the mushy zone is kinetically-limited (not convection-limited). The EMPA results, Figure 7, also indicate that a large amount of Pu is present in the Ta-Ti alloy globules to a surprisingly consistent level, about 25 wt.%, which may correspond to the location of the terminal β solid solution. If so, this would indicate a considerable extension of the β phase field towards the Pu corner of the ternary isotherm, since the terminal β-Ti and Ta phases are reported to only take 3 and ~0 wt.% Pu into solution at 850 °C, respectively (16). It is also possible that a ternary intermetallic phase intervenes, with a speculated composition of 35Ti-35Ta-25Pu (wt.%).

Other unexplained observations include the size distribution of the globules, both within a single specimen and between alloy compositions (Figure 9). The globule diameters are smaller nearer the bulk liquid suggesting slow dissolution. If this process is kinetically limited by diffusion of Ti and Ta, one would expect that the higher Ta alloys would diffuse more slowly due to their higher melting points. Since these alloys also have smaller grain sizes, it is logical that as the Ta content is increased a greater proportion of the attack will be confined to the grain boundary regions. While this is true for the case of the Ta-20 wt.% Ti alloy, it is not obvious in the Ta-40 wt.% Ti alloy.

Conclusions

1. The depth of corrosion increases with Ti content, although differences in grain size and other microstructural features may have exaggerated this trend.

2. Corrosion initially proceeds by intergranular attack to a depth of about 100 μm after which heterogeneous dissolution of the free grains takes place. The size of the free grain remnants and thickness of the resulting mushy zone increases with Ti content.

3. The solubility of Pu is greater in the Ta-60 wt.% Ti than in either pure Ta or Ti.

4. Liquid Pu at 850 °C can dissolve twice as much Ta from the Ta-60 wt.% Ti alloy compared with pure Ta. The evidence also suggests that the solubility of Ti from this alloy in Pu is decreased compared with pure Ti.

References

1. R.L. Andelin, L.D. Kirkbride and R.H. Perkins, Los Alamos Scientific Laboratory, "High-Temperature Environmental Testing of Liquid Plutonium Fuels," LA-3631 (1967).

2. K.M. Axler and E.M. Foltyn, Los Alamos National Laboratory, "High-Temperature Materials Compatibility Testing of Refractory Materials: TaC, Y_2O_3, Y_2O_3-Coated MgO, and BN," Report # LA-11586-MS (1989).

3. K.M. Axler, G.D. Bird and P.C. Lopez, "Evaluation of Corrosion Resistant Materials for Use in Plutonium Pyrochemistry," (Phoenix, AZ: Fall Mtg. The Electrochemical Society, 1991), Abstract No. 188.

4. K.M. Axler, et al., Processing and Characterization of Engineered Materials in the Tantalum Carbon System," H. Henein and T. Oki, eds., (Hawaii: First International Conference on Processing Materials for Properties, 1993), 221-223.

5. Plutonium Handbook, (New York: Gordon and Breach, Science Publishers, 1967), 592-593.

6. J.L. Murray, ed., "Phase Diagrams of Binary Titanium Alloys," in Monograph Series on Alloy Phase Diagrams, (Metals Park, Ohio, USA: ASM International, 1987) 302-306.

7. W.J. Tomlinson and R. Rushton, "The Fabricability and Hardness of Concentrated Binary Tantalum Alloys containing Titanium, Hafnium, Vanadium, Molybdenum, Tungsten, Rhenium and Palladium," J. Less-Common Metals, 115 (1986), L1-L4.

8. F.F. Schmidt, et al., Battelle Memorial Institute, "Investigation of the Properties of Tantalum and Its Alloys," WADD Technical Report # 61-106 (1961).

9. Y.S. Chen and C.J. Rosa, "Oxidation Characteristics of Ti-4.37 wt.% Ta Alloy in the Temperature Range 1258-1473 K," Oxidation of Metals, 14 (1980), 167-185.

10. J.D. Cotton, et al., unpublished work, Los Alamos National Laboratory, Los Alamos, NM 87545.

11. D.A. Prokoshkin, T.A. Voronova and A.S. Gorbova, "Kinetics of Oxidation of Ta-Ti Alloys," Iz. Akad. Nauk. SSSR (Metally), 5 (1984), 178-180.

12. R.F. Voytovich and E.I. Golovko, "Oxidation of Ti-Ta and Ti-Nb Alloys," Russ. Metally. USSR, 1 (1979), 183-187.

13. D.F. Bowersox and J.A. Leary, "The Solubilities of Carbon, Tantalum, Tungsten and Rhenium in Liquid Plutonium," J. Nucl. Mater., 21 (1967), 219-224.

14. D.R. Bowersox and J.A. Leary, "The Solubilities of Selected Elements in Liquid Plutonium II. Titanium, Vanadium, Chromium, Manganese, Zirconium, Niobium, Molybdenum and Thulium," J. Nucl. Mater., 27 (1968), 181-186.

15. M G. Fontana and N.D. Greene, Corrosion Engineering, (McGraw-Hill Book Co., 1978), 292.

16. F.H. Ellinger, et al., Los Alamos Scientific Laboratory, "Constitution of Plutonium Alloys," Report # LA-3870 (1968).